Brain Topogr (2008) 21:11–21
DOI 10.1007/s10548-008-0063-4

ORIGINAL PAPER

Parvocellular and Magnocellular Contributions to the Initial Generators of the Visual Evoked Potential: High-Density Electrical Mapping of the "C1" Component

John J. Foxe · E. Cathrine Strugstad · Pejman Sehatpour · Sophie Molholm · Wren Pasieka · Charles E. Schroeder · Mark E. McCourt

Accepted: 15 August 2008 / Published online: 11 September 2008

Abstract The C1 component of the VEP is considered to index initial afference of retinotopic regions of human visual cortex (V1 and V2). C1 onsets over central parieto–occipital scalp between 45 and 60 ms, peaks between 70 and 100 ms, and then resolves into the following P1 component. By exploiting isoluminant and low-contrast luminance stimuli, we assessed the relative contributions of the Magnocellular (**M**) and Parvocellular (**P**) pathways to generation of C1. C1 was maximal at 88 ms in a 100% luminance contrast condition (which stimulates both **P** and **M** pathways) and at 115 ms in an isoluminant chromatic condition (which isolates contributions of the **P** pathway). However, in a 4% luminance contrast condition (which isolates the **M** pathway), where the stimuli were still clearly perceived, C1 was completely absent. Absence of C1 in this low contrast condition is unlikely to be attributable to lack of stimulus energy since a robust P1–N1 complex was evoked. These data therefore imply that C1 may be primarily parvocellular in origin. The data do not, however, rule out some contribution from the **M** system at higher contrast levels. Nonetheless, that the amplitude of C1 to **P**-isolating isoluminant chromatic stimuli is equivalent to that evoked by 100% contrast stimuli suggests that even at high contrast levels, the **P** system is the largest contributor. These data are related to intracranial recordings in macaque monkeys that have also suggested that the initial current sink in layer IV may not propagate effectively to the scalp surface when **M**-biased stimuli are used. We also discuss how this finding has implications for a long tradition of attention research that has used C1 as a metric of initial V1 afference in humans. C1 has been repeatedly interrogated for potential selective attentional modulations, particularly in spatial attentional designs, under the premise that modulation of this component, or lack thereof, would be evidence for or against selection at the initial inputs to visual cortex. Given the findings here, we would urge that in interpreting C1 effects, a consideration of the dominant cellular contributions will be necessary. For example, it is plausible that spatial attention mechanisms could operate primarily through the M system and that as such C1 may not always represent an adequate dependent measure in such studies.

Keywords Event-related potential (ERP) · Magnocellular · Parvocellular · Striate cortex · Spatial attention · C1 component · Contrast-sensitivity

J. J. Foxe · S. Molholm · C. E. Schroeder
Program in Cognitive Neuroscience, Department of Psychology, The City College of the City University of New York, 138th St. & Convent Avenue, New York, NY 10031, USA

J. J. Foxe (✉) · E. C. Strugstad · P. Sehatpour · S. Molholm · C. E. Schroeder
The Cognitive Neurophysiology Laboratory, Program in Cognitive Neuroscience and Schizophrenia, Nathan S. Kline Institute for Psychiatric Research, 140 Old Orangeburg Road, Orangeburg, NY 10962, USA
e-mail: foxe@nki.rfmh.org

E. C. Strugstad · P. Sehatpour
Ferkauf Graduate School of Psychology, Albert Einstein College of Medicine, 1165 Morris Park Avenue, Bronx, NY 10461, USA

W. Pasieka · M. E. McCourt
Center for Visual Neuroscience, Department of Psychology, North Dakota State University, Fargo, ND 58105, USA

Introduction

One of the earliest visual evoked potential (VEP) components detectable through scalp recordings has been termed the C1 (Jeffreys and Axford 1972). This component typically

onsets over central parieto–occipital scalp between 45 and 60 ms post-stimulus, peaks between 70 and 90 ms, and then resolves into the following P1 component. It is now well-established that this component receives its largest contributions from the earliest retinotopic regions of the visual processing hierarchy, particularly V1 but likely also from V2 (e.g. Clark and Hillyard 1996; Martinez et al. 1999; Foxe and Simpson 2002). The retinotopic organization of area V1 is such that stimuli presented to the lower visual field are mainly projected to the upper bank of the calcarine fissure, while upper field stimuli project to its lower banks. Scalp ERP recordings have demonstrated that the C1 polarity reverses depending on the presentation of stimuli to the upper or lower visual fields, with upper field presentations producing a C1 that manifests as scalp negativity and lower field presentations producing a scalp positivity (e.g. Di Russo et al. 2003; Kelly et al. in press). This geometry-dependent behavior of the C1 provides strong support for the localization of the major generators of the C1 to the primary visual area V1, which is the only region with a geometric configuration that would produce such a pattern. Source-analysis of ERP data has also confirmed that V1 is the major generator of this component (e.g. Gomez-Gonzalez et al. 1994; Simpson et al. 1995a, b; Clark et al. 1995; Ikeda et al. 1998; Di Russo et al. 2002).[1] Although the use of quadrant-delimited stimuli is the optimal way to evoke the C1, central presentations can also result in a robust C1 that manifests as a scalp negativity (e.g. Foxe and Simpson 2002; Molholm et al. 2002; Foxe et al. 2003; McCourt and Foxe 2004).

A key question concerns the relative contributions of the major visual cellular subsystems to the generation of this component. Primary visual cortex receives parallel inputs from two major cellular subtypes, the so-called parvocellular (**P**) and magnocellular (**M**) systems (Ungerleider and Mishkin 1982; Van Essen and Maunsell 1983). These two systems subserve different functions and carry different and segregated inputs into cortex. Magnocellular cells, named for their large axons, are fast conducting neurons that provide the rapid initial afferent input to primary visual cortex. They have large receptive fields and are particularly sensitive to low spatial frequency and moving stimuli (see Livingstone and Hubel 1988). They also respond well to low contrast stimuli but are entirely "blind" to chromatic stimuli that lack a luminance component (Kaplan 1991; Merigan and Maunsell 1993). The parvocellular system on the other hand contains cells with smaller cell bodies and hence their axons conduct more slowly. These cells respond better to detailed high spatial frequency inputs and are best driven by higher contrast stimuli. In fact, it is believed they are essentially "blind" to contrast levels below about 8% (Tootell et al. 1988a, b). On the other hand, they are highly sensitive to chromatic contrast stimuli, unlike **M** cells, even in the absence of any luminance component (e.g. Merigan 1989).

Here, we set out to determine the respective contributions of the parvocellular and magnocellular systems to the generation of the C1 component of the VEP. For this purpose we used stimuli that selectively target magnocellular and parvocellular divisions of the visual pathway. Determining the respective contributions of **M** and **P** systems to a given VEP component may have important clinical implications. For instance, selective deficits within one or the other cellular system have been posited for a number of clinical populations, such as putative magnocellular deficits in dyslexia (e.g. Livingstone et al. 1991) and schizophrenia (e.g. Schwartz et al. 2001; Butler et al. 2001, 2007; Foxe et al. 2001, 2005a, b; Yeap et al. 2006; Lalor et al. 2008). This question also has important implications for estimating the onset timing of inputs to human visual cortex. For example, if the C1 represents only parvocellular inputs, then onset estimates previously made on the basis of this component have likely overestimated the timing of initial afference in V1 since the **P** system is considerably slower than the **M** system (see Schroeder et al. 1998, 2001). Here we use high-density ERP recordings from 168 scalp channels to detail the spatio-temporal dynamics of C1 generation under selective **P** and **M** stimulation conditions.

Materials and Methods

Participants

Eleven (5 female) neurologically normal, paid volunteers (ages 19–45 years, mean 29.2 years) participated. All participants provided written informed consent, and the Institutional Review Board of the Nathan Kline Research Institute approved all procedures. All participants reported normal or corrected-to-normal vision and were right-handed, as measured using the Oldfield laterality inventory (Oldfield 1971). All participants were screened with the Ishara test of colorblindness.

Stimuli

We used three types of stimuli: 100% contrast stimuli (targeting both **M** and **P** streams), 4% contrast stimuli (targeting **M** cells alone) and red–green isoluminant stimuli

[1] It should be pointed out that while the C1 shows a generally "retinotopic" pattern of reactivity, the picture is rather more complex. The timing of sensory transmission through the visual system is very rapid and many regions of the visual system are necessarily activated during the timeframe of the C1. In line with this timing, Foxe and Simpson (2002) showed that the C1 also received contributions from extrastriate cortical regions.

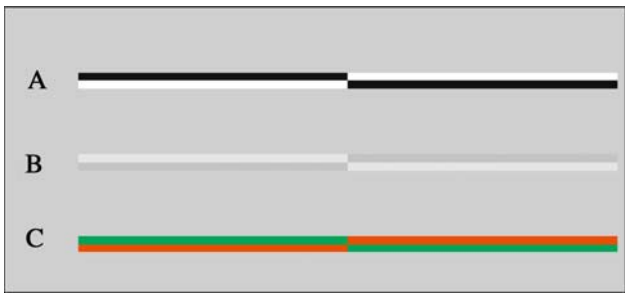

Fig. 1 Illustration of the line stimuli used in the experiment: (**A**) 100% contrast stimuli (targeting both **M** and **P** streams), (**B**) 4% contrast stimuli (targeting **M** cells alone) and (**C**) red–green isoluminant stimuli (targeting **P** cells alone). Lines subtended 14.03° in width and 0.12° in height

(targeting **P** cells alone). The stimuli consisted of elongated rectangular stimuli that subtended 14.03° in width and 0.12° in height. These rectangles were presented centrally with the long axis oriented along the horizontal meridian. Each rectangle was broken into four quadrants (7° × 0.06°), which were filled in a checkerboard fashion (see Fig. 1). Stimuli were presented tachistoscopically for 150 ms on an Iyama model-512 21-in. CRT, dot pitch of 0.24, resolution 1280 × 1024 pixels, frame refresh rate of 85 Hz and mean display luminance was 100 cd/m^2. Viewing distance was 108 cm.

For the isoluminant chromatic condition, red–green isoluminance was determined on a subject-by-subject basis using flicker photometry (Kaiser 1979). Red and green levels were also made equiluminant with the gray background by flicker photometry before testing began. Flicker photometry utilizes the fact that the chromatic system is too slow to follow fast temporal changes whereas the luminance system is able to detect the fast changing luminance differences between a given pair of colors. Therefore, if the perception of flicker is eliminated, the luminance component can be eliminated too. The flicker stimuli in our test sequence consisted of a rectangular patch divided into two equal segments differing in color. Each color segment alternated between red and green at 20 Hz. Each segment was 2.12° by 2.12° visual angle. Red was kept constant at the maximum intensity of the cathode ray tube (CRT). Participants were instructed to adjust the intensity of the green patch until the perception of flicker was judged to be minimal. They performed 10 such judgments. The largest and smallest values were then discarded and the 8 remaining values were averaged to determine a given subject's subjective equiluminance point. The procedure was also repeated for each color in combination with the grey background. All participants reported that they could find a setting where the flicker disappeared.

The stimuli were presented to participants in the context of a demanding line-bisection task. A detailed description of the task is provided in a previous publication from this laboratory (Foxe et al. 2003), but note that these are not data from that experiment. In the present analysis, only early sensory processing is assessed and these early components are not modulated by the bisection task. One major benefit of using a demanding task such as this to assess early sensory function is that the general arousal level of the subject is controlled for. We plan to report later attention-related effects from this manipulation in a future manuscript.

Electrophysiological Measures

Continuous EEG was acquired through the ActiveTwo Biosemi™ electrode system from 168 scalp electrodes, digitized at 512 Hz. For display purposes, data were filtered with a 40 Hz low-pass, 0-phase shift, 96 dB per octave filter after acquisition. With the Biosemi system, every electrode or combination of electrodes can be assigned as the "reference", and this is done purely in software after acquisition (For a detailed description of the referencing and grounding conventions used by this active electrode system, the reader is referred to the following website: http://www.biosemi.com/faq/cms&drl.htm.

All data were re-referenced to a frontal electrode (FPz) after acquisition. Data were epoched off line from 100 ms pre-stimulus to 400 ms post-stimulus and baseline-corrected from 100 ms pre-stimuli to 0 ms. Trials with blinks and eye movements were rejected on the basis of horizontal and vertical electrooculogram. At all scalp sites, trials with excessive EEG or noise transients were rejected by applying an artifact rejection criterion of ±60 μV. From the remaining artifact-free trials, averages were computed for each subject. These averages were then visually inspected for each individual to ensure that clean recordings with sufficient numbers of trials were obtained and that no artifacts were still included. The average number of accepted trials per condition across participants was 405 (SD = 66.9). Traditional ERP componentry over posterior scalp were identified from group-averaged waveforms.

Scalp ERP Waveform Analysis

The topography of C1 has been well characterized by previous studies and was found to be highly similar here. Figure 2 shows the scalp topography of C1 for the 100% contrast, the isoluminant chromatic and the 4% contrast conditions. Guided by the scalp topographic mapping, the ERP waveforms recorded from the electrodes that maximally reflected the activity from the C1 generators were plotted and further interrogated.

To statistically test for the onset and presence of a significant C1 deflection, we employed two approaches. In the first, we took the baseline to be an accurate representation

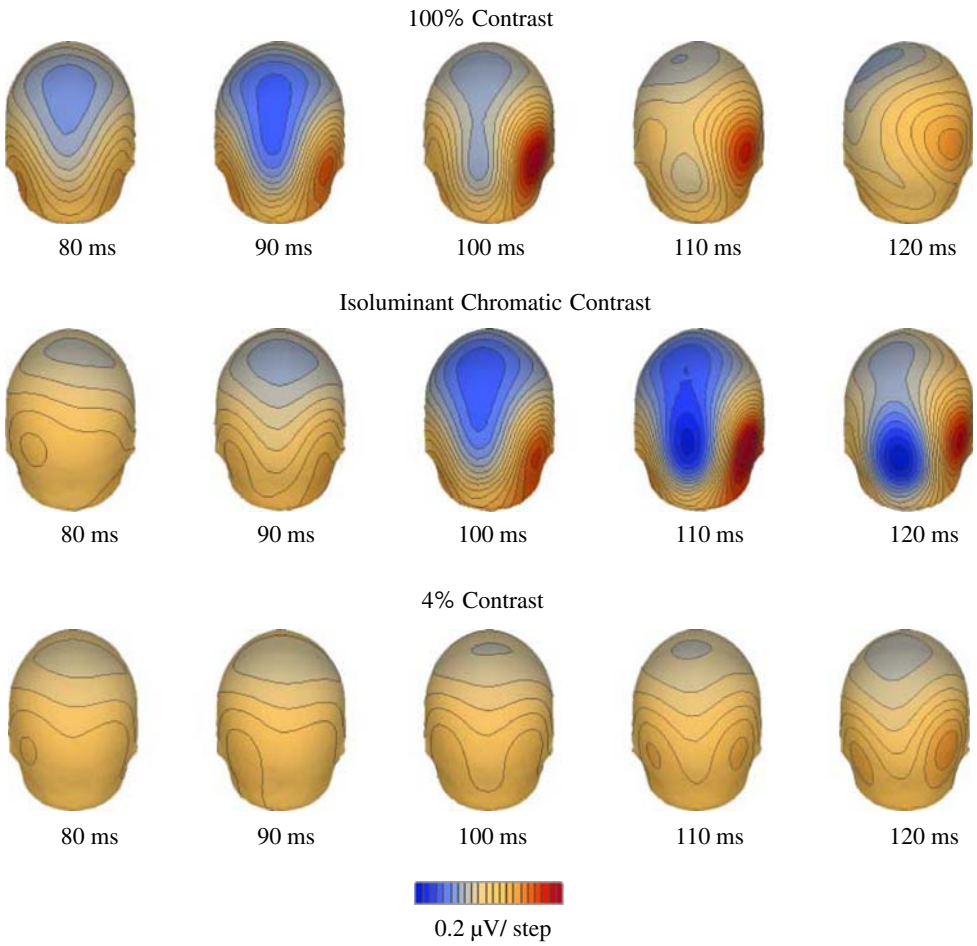

Fig. 2 Voltage maps of the group-averaged data extending from 80 to 120 ms post-stimulus for the three experimental conditions: 100% contrast, isoluminant chromatic, and 4% contrast. This map progression spans the timeframe of the C1 component (midline negativity). The midline negativity was evident in the case of the 100% contrast and isoluminant chromatic contrast conditions; however it was absent in the 4% contrast condition

of noise in the data, both within and across subjects. A composite *P*-value was determined for each time-point from 40 ms post-stimulus onwards by averaging the *P*-values obtained across 12 paired two-tailed *t*-tests each comparing that time point with one of 12 pre-stimulus time points (every other data point in the interval −50 to 0 ms). These composite *P*-values give us a measure of significant deviation from baseline for every time point starting from 40 ms post-stimulus. A statistically significant deflection from the baseline was considered only when at least eight consecutive significant ($P < 0.05$) data points were obtained (Guthrie and Buchwald 1991).

We also performed a 3 × 3 repeated measures ANOVA with factors of stimulus type (100%-contrast, Isoluminant-Chromatic, 4%-contrast) and electrode site (the three midline occipital scalp sites that best represented the C1, as shown in Fig. 4). The dependent measure was an integrated area measure (versus the 0 μV baseline) for each of the three conditions, which were derived for a window of 8 time-points spanning the observed peak C1 amplitude in the group-averaged data. Note that in the case of the 4% condition, no peak was discernable so measures were made for the same timeframe as the isoluminant condition.

Scalp Current Density Mapping (SCD)

To better define the scalp-topographic distribution of the C1 we used the SCD or surface Laplacian transformation. In this technique, the second spatial derivative of the scalp potential is computed from the spherical spline interpolation of the voltage recordings (Perrin et al. 1987). This approach eliminates the influence of the electrical reference and also minimizes the effect of the voltage gradients due to tangential current flow within the scalp. The advantage of this mapping technique is that it emphasizes local contributions to the surface map, hence providing a better approximation of the intracranial generators.

Results

Our experimental design enabled us to tease apart the contribution of the M and the P pathways to the C1 component.

Figure 2 shows voltage maps of the group-averaged data extending from 80 to 120 ms post-stimulus for the three conditions of this experiment: 100% contrast, isoluminant

chromatic, and 4% contrast. This map progression spans the timeframe of the C1 component. The initial segment of the C1 has a clear focus over the midline parieto–occipital scalp region, as is typically found, which then propagates somewhat more inferiorly to the central occipital scalp. In both Fig. 2 and the waveforms plotted in both Figs. 3 and 4, a clear C1 component is evident for the 100% contrast condition (Parvo + Magno) and for the isoluminant chromatic stimulus condition (Parvo alone). However, this component appears to be entirely absent in the 4% contrast condition (Magno alone).

The ERP waveforms recorded from three midline electrode sites that maximally reflected activity from the C1 generators (see Fig. 4) were submitted to statistical testing as outlined above. Table 1 indicates the results for each of the three conditions. Robust C1s were found for the 100% contrast and isoluminant chromatic conditions but this analysis indicated no significant deviations from the baseline for the 4% contrast condition in the timeframe preceding the P1 component, a fact that is obvious from simple observation of the waveforms in Fig. 3.

The peak amplitude of C1 was found to be at 88 ms for the 100% condition and at ~115 ms for the isoluminant chromatic condition. Inspection of the waveforms at the central occipital scalp-site (Oz) reveals that the peak of the C1 component for the 100% condition precedes the peak of the C1 for the color condition by approximately 30 milliseconds.

Figure 5 shows the SCD map at the peak of the C1 component for the 100% contrast condition occurring at 88 ms and for the isoluminant chromatic condition occurring at 116 ms. The reader will appreciate that the topographies show extremely similar distributions.

A 3 × 3 ANOVA with factors of stimulus type (100%-contrast, Isoluminant-Chromatic, 4%-contrast) and

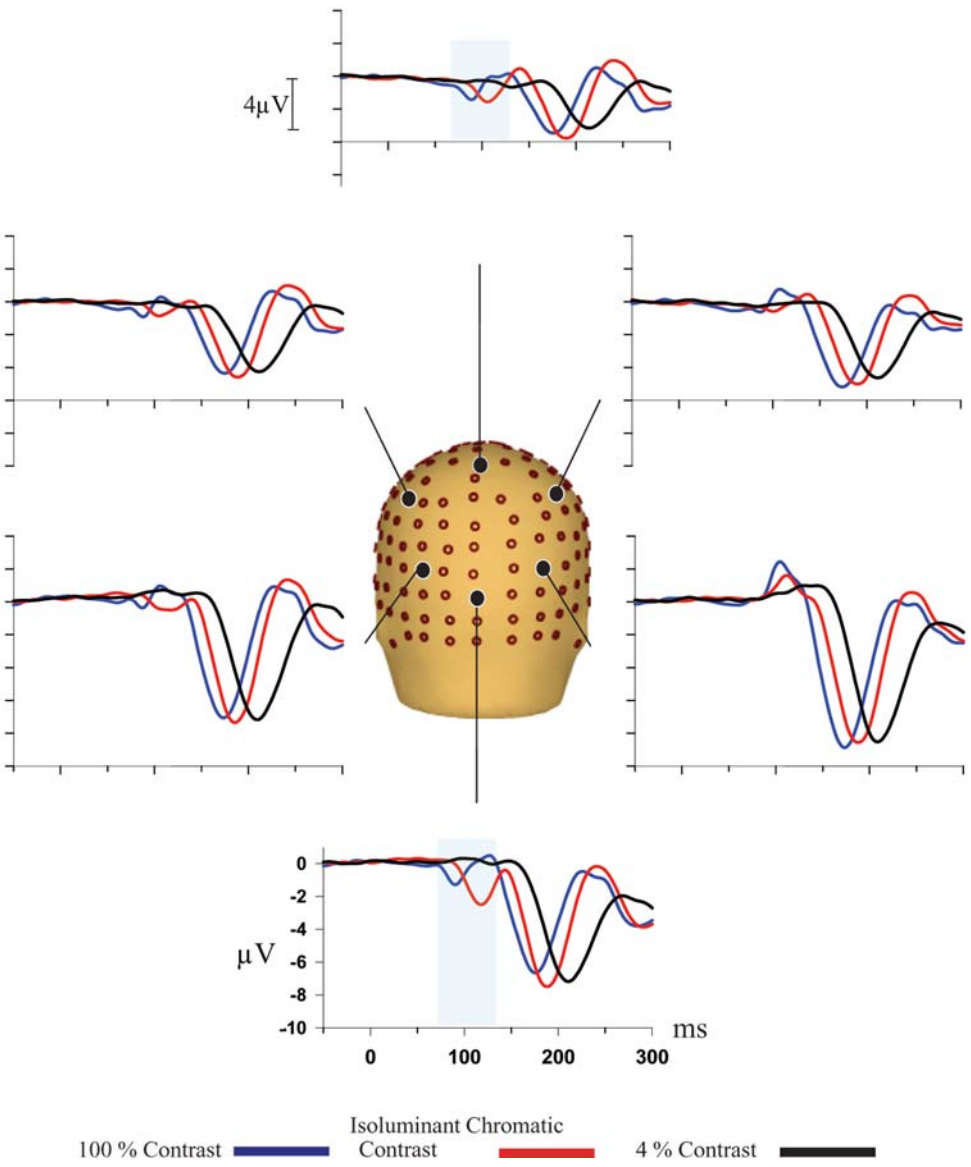

Fig. 3 The ERP waveforms recorded from a selection of posterior parietal and occipital electrode-sites illustrate the general VEP response patterns seen to these line stimuli. The recordings show waveforms derived for each of the experimental conditions, namely 100% contrast, isoluminant chromatic, and 4% contrast. The light cyan shading indicates the general timeframe of the C1 processing period

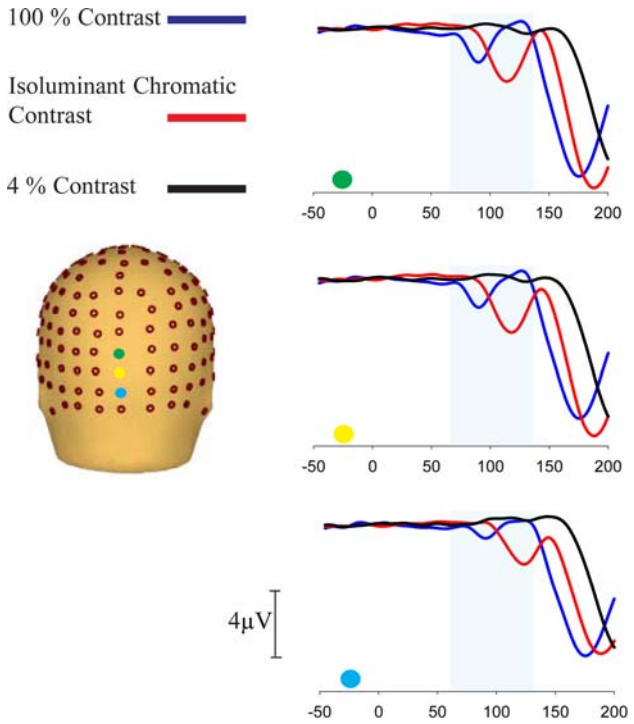

Fig. 4 Waveforms are shown for the three midline occipito-parietal scalp sites that maximally reflected activity from the C1 generators. Measures from these sites were used in statistical analyses (see Table 1 also). The light cyan shading indicates the general timeframe of the C1 processing period

Table 1 The timeframes during which the C1 was significantly present are delineated in this table for the three main conditions (100% contrast, Isoluminance, 4% contrast)

Scalp site	Significant time-window (ms)	Peak latency (ms)	*P*-value at peak
100% contrast condition			
Green	79–97	88	0.01
Yellow	81–95	88	0.01
Blue	ns	–	ns
Isoluminant chromatic condition			
Green	97–126	117	0.007
Yellow	101–128	115	0.005
Blue	107–128	115	0.005
4% contrast condition			
Green	ns	–	ns
Yellow	ns	–	ns
Blue	ns	–	ns

Note that "Green", "Yellow" and "Blue" refer to the corresponding electrode locations plotted on the scalp in Fig. 4

electrode site (the three midline occipital scalp sites that best represented the C1) was also conducted. A main effect of stimulus type was found to be significant ($F_{1,10} = 5.798$, $P = 0.01$). A series of 2×3 protected-ANOVAs were

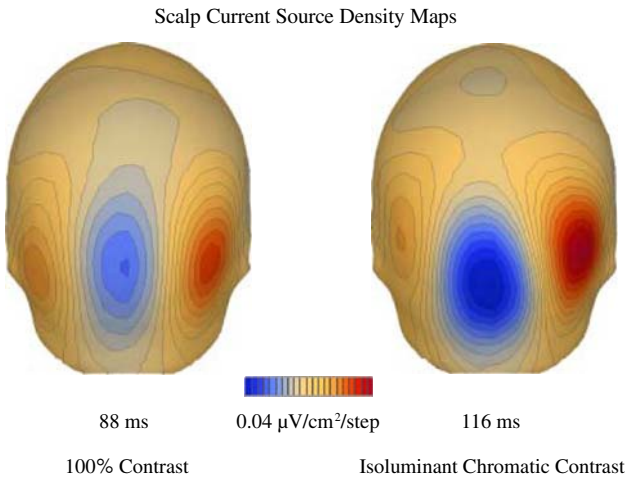

Fig. 5 Scalp Current Density (SCD) maps at the peak of the C1 component for the 100% contrast condition occurring at 88 ms and for the isoluminant chromatic condition occurring at 116 ms (see Table 1) illustrate the highly similar topographies of this component across the two conditions

conducted to unpack this effect of stimulus. The contrast of the 100% with the 4% condition was significant ($F_{1,10} = 9.584$, $P = 0.011$), as was the contrast of Isoluminant with 4% ($F_{1,10} = 7.867$, $P = 0.019$). The contrast of the 100%-contrast condition with the isoluminant condition was not reliable ($F_{1,10} = 1.924$, $P = 0.2$).

Discussion

Disentangling M, P and K Pathway Contributions to C1

By exploiting both isoluminant and low contrast luminance stimuli we have attempted to reveal the relative contributions of the **M** and the **P** pathways to the C1 component of the visual evoked potential (VEP). We found that C1 amplitude was maximal at electrode sites over the occipital cortex at latencies of 88 ms in the 100% luminance contrast condition (which indexes the response of both **P** and **M** pathways) and at 115 ms in the isoluminant chromatic condition (which isolates the contribution of the **P** pathway). Especially noteworthy was the complete absence of C1 evoked in the 4% luminance contrast condition (which isolates the **M** pathway). The absence of the C1 component in this low contrast condition cannot be attributed to a simple lack of stimulus energy since robust P1 and N1 components were elicited in response to these stimuli, and as we will discuss in more detail below, the **M** system is vigorously activated by contrast levels similar to those used here (Shapley et al. 1981). These data therefore strongly imply that the C1 component of the VEP is primarily parvocellular in origin. In support, a recent paper aimed at studying **M** and **P** contributions to the VEP in patients with

schizophrenia showed a highly similar pattern of results to those reported here (Schechter et al. 2005).

While the amplitude of C1 does not reliably differ between the 100% contrast and isoluminant conditions, C1 latency is considerably shorter (by approximately 30 ms) in the 100% contrast condition. This latency difference is consistent with the well-known decrease in response latencies of retinal and LGN neurons with increasing stimulus luminance (Schroeder et al. 1989; Maunsell et al. 1999). Alternatively P-cells with strong spectral opponency might respond more sluggishly than those with weak opponency. Of course, another possibility is that during the higher contrast condition, we have begun to see the effects of Magnocellular responsivity in the C1, and this is a possibility that we simply cannot rule out with the current dataset. Nonetheless, that the amplitude of C1 to **P**-isolating isoluminant chromatic stimuli is equivalent to that evoked by 100% contrast stimuli suggests that even at high contrast levels, the P system is the largest contributor. If a major **M** contribution were suspected, one would surely predict a substantial increase in C1 amplitude to reflect both **M** and **P** contributions. As we will come to below, there are further reasons to doubt a major **M** contribution. Clearly though, additional experiments will be necessary to fully account for the latency differences we report.

Finally, it has recently been suggested that the koniocellular (K) system, long identified with the blue-yellow chromatically opponent system, might also subserve the processing of red–green chromatic opponency (Calkins and Sterling 1999). Thus, another interpretation of the C1 latency difference observed in response to red–green isoluminant and 100% luminance contrast stimuli is that the former might be mediated by the K-pathway whereas the latter represent P-pathway activity. The proposition that the K-pathway supports red–green opponency has not enjoyed support (Chatterjee and Callaway 2003), making this an unlikely explanation for the latency differences we observe. It would, however, be of interest to measure C1 amplitude and latency in response to yellow–blue isoluminant contrast stimuli in order to assess possible K-pathway contributions.

The Cellular/Laminar Substrates of the "C1"

This issue was investigated in earlier experiments that entailed recordings in awake behaving monkeys using linear array multi-electrodes that could record simultaneously from all of the layers of a visual cortical region (Schroeder et al. 1991, 1997, 1998; Givre et al. 1995). These experiments identified a surface-negative component, termed N40 because it peaks at 40 ms latency under high intensity conditions. N40 seems very likely to be the simian homologue of the human C1. All of these studies agree on the essential point that N40 is generated primarily by discharge of thalamo-recipient spiny stellate neurons in Lamina 4C, although there does also seem to be some contribution from the synchronous discharge of thalamo-cortical afferent terminals (Tenke et al. 1993). Subsequent studies suggested that N40 receives relatively little contribution from extrastriate visual areas (Givre et al. 1994; Schroeder et al. 1998). Use of wavelength limited stimulation, which causes a bias of effective activation toward the **P** system, causes a dramatic increase in both the amplitude and the latency of the N40, so that its peak latency shifts to between 50 and 60 ms post-stimulus (Givre et al. 1995).[2] These effects parallel those found with isoluminant stimulation in the present study, insofar as the latency of the C1 increases substantially, although the amplitude does not increase. Although the M-recipient, as well as the P-recipient subdivisions of Layer 4C of V1 are activated by most stimuli, there is indication from the modeling experiments (Tenke et al. 1993) that the deeper portions of Layer 4C (i.e. the P-recipient zone), along with the grouped thalamic afferent discharge, are the most critical neural substrates for the N40 component. Thus, in the low contrast condition the N40 contribution from the M-recipient division of Layer 4C may be masked by positive potentials generated by current flow in more superficial layers, a process which does seem to occur in some cases with pattern stimulation (Schroeder et al. 1991). The effect would be to create a macroscopic closed-field whereby distant electrodes such as those at the scalp would be insensitive to either source of activity.

Implications of a Parvocellular Origin of the "C1" for Attention Research

The C1 component has been central to a major ongoing debate in the human attention literature and as such its cellular substrates are of considerable import to this issue. A fundamental question in theories of selective attention is the level of processing at which selection occurs, with some positing late selection (e.g. Deutsch and Deutsch 1963; Driver and Tipper 1989; see Driver 2001 for a nice review) and others contending that selection occurs very early in sensory processing (e.g. Broadbent 1958; Lachter et al. 2004; Kelly et al. in press). As the putative metric of initial V1 afference, the C1 has been repeatedly

[2] The reader will note that the latencies of C1 in macaques are considerably shorter than those in humans across the various stimulus classes. This is a commonly observed phenomenon and has been discussed extensively in previous work (see Foxe and Schroeder 2005). That is, across a wide variety of visual, auditory and somatosensory response measures, macaque monkey latency values have been found to be about 3/5 the corresponding ones in humans (see Schroeder et al. 1998). For example, the macaque pattern-evoked visual P1 component peaks at 60 ms, while the human P1 typically peaks at 100 ms (Schroeder et al. 1991).

interrogated for potential selective attentional modulations, particularly in spatial attentional designs, under the premise that modulation of this component would be evidence for selection at the initial inputs to visual cortex. In the human ERP literature, the C1 has proven, to a great extent, to be fairly immune to modulation under a variety of selective attentional designs (e.g. Hillyard et al. 1998; Martinez et al. 1999, 2001; Noesselt et al. 2002; Hillyard and Anllo-Vento 1998) and so for quite some time, it became fairly widely accepted that selection did not occur at the level of initial V1 afference.[3] More recent work has since shown that processing during the initial phase of C1 is indeed modulated by spatial attention (Kelly et al. in press), but even so, the modulation is relatively modest.

Crucially, if C1 is mostly or even wholly driven by the parvocellular system, as the present data suggest, should this potentially change our interpretation of attention studies that have looked to C1 as evidence for the lack or near-lack of early attention effects? One might begin by asking which cellular system, **P** or **M**, is most likely to be the target of influences from spatial attention? Since **M** cells provide the primary projection to the dorsal visual stream (see Merigan and Maunsell 1993), the so-called "where" processing stream implicated in visuo-spatial processing, it seems at least plausible that spatial attention mechanisms might operate primarily through re-entrant modulations of activity in the **M** system. Data from functional imaging (Coull and Nobre 1998; Gitelman et al. 1999), electrophysiology (e.g. Foxe et al. 1998, 2003, 2005a, b; Foxe and Simpson 2005; Dale et al. 2008) and of course, from hemi-spatial neglect patients (e.g. Heilman and van den Abell 1980; Vallar and Perani 1986, 1987) have clearly implicated dorsal stream visual areas in the control of spatial attention mechanisms. As such, if it is true that spatial attention is more likely to target **M** inputs, a VEP component driven largely or exclusively by **P** inputs may not have been the best metric for assessing early V1 attention effects. Of course, this is an empirical issue that should be readily testable using **P** versus **M** biased stimuli in a spatial attention paradigm.

We acknowledge that the present data do not entirely rule out the possibility of some **M**-system contribution to C1 at higher stimulus contrast. This caveat is pertinent because high-contrast stimuli were typically used in the previously mentioned spatial attention paradigms. That high-contrast stimuli evoke both **P** and **M** responses makes dissociating their relative contributions to scalp-recorded potentials problematic if not impossible. That **M**-system responses might contribute to C1 amplitude at high stimulus contrasts is supported by the neuroimaging experiments of Tootell et al. (1995, 1998) who used fMRI to describe a steep contrast-gain function for area V1 but curiously failed to find a significant hemodynamic signal at stimulus contrasts below 6%. On this basis it could be argued that our 4% contrast stimulus was too weak to evoke a robust **M**-system response. The findings of Tootell et al. (1995, 1998), however, are themselves inconsistent with the more directly relevant intracranial electrophysiological recordings from primate lateral geniculate nucleus (Shapley et al. 1981; Derrington and Lennie 1984; Kaplan and Shapley 1986) which have shown that **M** cells have very high contrast-gain and reach their half-saturation response rates at very low contrast levels with vigorous responding seen at 4% contrast and below [see Fig. 30.5 in Ref. Kaplan and Shapley (1986)]. Extracellular recordings from the **M**-recipient layers of V1 reveal similar results. Hubel and Livingstone (1990) measured the contrast-response of neurons in monkey area V1 and noted that the mean (and range) of the half-saturation constant of cells recorded from the **M**-recipient layers (4B and 4C-alpha) were nearly identical to those of neurons recorded from the magnocellular layers of the LGN, thus indicating a predominantly magnocellular source of input. The upshot of these intracranial results is that it seems very unlikely that the complete absence of a C1 in the 4% condition here can be accounted for in terms of muted activation of the **M** divisions of V1.

Additional EEG and MEG Evidence

A clear limitation of the present study is that only two contrast levels at opposite ends of the intensity scale were used and thus, we could not assess the contrast-gain function of the C1 across a range of contrast levels to see if its gain function was also consistent with mainly **P** inputs. The use of just three discrete stimulus classes here was motivated by our wish to collect large numbers of trials of each type so that signal-to-noise ratios would be as high as possible. The contrast gain function of the visual evoked potential (or evoked field) has, however, been studied. Ellemberg et al. (2001) investigated the interaction of spatial frequency and contrast on the early VEP componentry using contrast reversing sinusoidal gratings and a single channel recording from a midline occipital scalp-site (Oz). They found that the C1[4] was evoked only at

[3] It should be noted that although selection was not seen during this "earliest" component in these studies, it was seen very quickly thereafter during the initial phases of the P1 component (80 ms onwards) and this has been taken as indication of relatively early spatial selection (e.g. Mangun et al. 2001).

[4] Note that Ellemberg refers to the first VEP negativity as N1, following a nomenclature in equally common use in the literature (e.g. Kubová et al. 1995). We prefer the use of the term C1 simply because of the retinotopic behavior of this component, since it can be seen as both a scalp positivity and a scalp negativity dependent on the location of the stimulus in the upper or lower visual field (e.g. Clark et al. 1995; Kelly et al. in press). It is generally more common in the cognitive neuroscience literature to refer to the bilateral negativity that follows P1, which typically peaks between 130 and 200 ms, as the "N1".

medium and high contrast stimulation levels (i.e. at 11% contrast and higher) and its amplitude increased slowly with increasing contrast such that it didn't saturate, a pattern that is entirely consistent with a **P** account for this component. On the other hand, the following P1 component showed a contrast-gain pattern that was more consistent with **M** functioning, since it was already evident at 4% contrast, and its amplitude increased rapidly up to 16% contrast, at which point it leveled off (saturated). Further, the C1 was also found to increase with increasing spatial frequency, again consistent with a **P** account. Similarly, in a magneto-encephalographic (MEG) study (Hall et al. 2005), the contrast gain function in V1 was investigated using the so-called "Beamformer" method to localize the intracranial generators of the early visual evoked fields (VEFs). These authors localized a striate source that showed a near linear contrast-gain function that didn't saturate (**P**-like), whereas a neighboring extrastriate source showed a saturating (**M**-like) function. A caveat here though is that the activity of the striate source was estimated over a 300 ms time-window so their assessment was not limited to the timeframe of the initial C1 component. Nonetheless, both of these studies of the contrast gain function in striate cortex also point to a largely **P** origin for the early striate response.

What then of the initial **M** response in V1 and is it the case that researchers using scalp-recorded measures will simply not be able to assay this response? We have recently developed a novel method of evoking visual responses that does not require the use of transient discrete stimulation, as is necessary for evoking the VEP. This response, which we have termed the VESPA (for Visual Evoked Spread Spectrum Analysis), is obtained using continuous, rapidly modulated stimuli (Lalor et al. 2006, 2007) and it is based on the assumption that the EEG response to a stimulus, whose luminance or contrast is rapidly modulated by a stochastic signal, consists of a convolution of that signal with an unknown impulse response. Given the known stimulus signal and the measured EEG, this impulse response can be estimated using the method of linear least squares. Using luminance modulation within the range of the **M** system (0–10%), we were able to elicit a robust C1 component with an onset latency that preceded the C1 evoked to **P**-biased stimulation (Lalor and Foxe in press), exactly as one would expect for the faster **M** system. Thus, the VESPA represents at least one method by which early **M** afference in V1 can be assessed.

Conclusions

Through the use of isoluminant and low-contrast stimuli, we assessed the relative contributions of the Magnocellular (**M**) and Parvocellular (**P**) pathways to generation of the classic C1 component of the VEP, a component that is well-accepted as an index of initial sensory processing within retinotopically mapped visual cortical areas (namely V1 and probably also V2). C1 was maximal at 88 ms in a 100% luminance contrast condition, a condition that vigorously stimulates both the **P** and **M** pathways. Using isoluminant chromatic stimulation, a condition that effectively isolates contributions from the **P** pathway, a clear C1 with a perfectly typical scalp topography was seen at 115 ms. However, in a 4% luminance contrast condition that isolates the **M** pathway, where the stimuli were clearly perceived, the C1 was found to be completely absent. These data therefore imply that C1 may be primarily parvocellular in origin, although they do not rule out some contribution from the **M** system at higher contrast levels. Nonetheless, that the amplitude of C1 to **P**-isolating isoluminant chromatic stimuli was found to be equivalent to that evoked by 100% contrast stimuli suggests that even at high contrast levels, the **P** system is likely to be the largest contributor. For those researchers using the C1 as their major dependent measure, such as those wishing to assess early attentional selection mechanisms, it will be important to consider the potential implications of the underlying cellular contributions to the C1.

Acknowledgements We would like to thank Dr. Vance Zemon, Dr. Barbara Blakeslee and Dr. Simon Kelly for very helpful discussions. We would like to especially thank Ms. Jeannette Mahoney, Ms. Marina Shpaner and Ms. Beth Higgins for their expert data collection. We would also like to acknowledge the passing of our friend and colleague, Brian "Wren" Pasieka, who is sorely missed. This work was supported by an NIMH RO1 grant to JJF (MH65350) and MEM received support from NCRR grant P20 RR020151.

References

Broadbent DE (1958) Perception and communication. Pergamon, London

Butler PD, Schechter I, Zemon V, Schwartz SG, Greenstein VC, Gordon J, Schroeder CE, Javitt DC (2001) Dysfunction of early-stage visual processing in schizophrenia. Am J Psychiatry 158(7):1126–1133

Butler PD, Martinez A, Foxe JJ, Kim D, Zemon V, Silipo G, Mahoney J, Shpaner M, Jalbrzikowski M, Javitt DC (2007) Subcortical visual dysfunction in schizophrenia drives secondary cortical impairments. Brain 130(Pt 2):417–430

Calkins DJ, Sterling P (1999) Evidence that circuits for spatial and color vision segregate at the first retinal synapse. Neuron 24:313–321

Chatterjee S, Callaway EM (2003) Parallel colour-opponent pathways to primary visual cortex. Nature 426:668–671

Clark VP, Hillyard SA (1996) Spatial selective attention affects early extrastriate but not striate components of the visual evoked potential. J Cogn Neurosci 8:387–402

Clark VP, Fan S, Hillyard SA (1995) Identification of early visual evoked potential generators by retinotopic and topographic analyses. Hum Brain Mapp 2:170–187

Coull JT, Nobre AC (1998) Where and when to pay attention: the neural systems for directing attention to spatial locations and to time intervals as revealed by both PET and fMRI. J Neurosci 18(18):7426–7435

Dale CL, Simpson GV, Foxe JJ, Luks TL, Worden MS (2008) ERP correlates of anticipatory attention: spatial and non-spatial specificity and relation to subsequent selective attention. Exp Brain Res 188:45–62

Derrington AM, Lennie P (1984) Spatial and temporal contrast sensitivities of neurones in lateral geniculate nucleus of macaque. J Physiol 357:219–240

Deutsch JA, Deutsch D (1963) Attention: some theoretical considerations. Psychol Rev 70:80–90

Di Russo F, Martínez A, Sereno MI, Pitzalis S, Hillyard SA (2002) Cortical sources of the early components of the visual evoked potential. Hum Brain Mapp 15:95–111

Di Russo F, Martinez A, Hillyard SA (2003) Source analysis of event-related cortical activity during visuo-spatial attention. Cereb Cortex 13(5):486–499

Driver J (2001) A selective review of selective attention research from the past century. Br J Psychol 92(I):53–78

Driver J, Tipper SP (1989) On the nonselectivity of "selective" seeing: contrasts between interference and priming in selective attention. JEP: HPP 15:304–314

Ellemberg D, Hammarrenger B, Lepore F, Roy MS, Guillemot JP (2001) Contrast dependency of VEPs as a function of spatial frequency: the parvocellular and magnocellular contributions to human VEPs. Spat Vis 15(1):99–111

Foxe JJ, Schroeder CE (2005) The case for feedforward multisensory convergence during early cortical processing. NeuroReport 16:419–423

Foxe JJ, Simpson GV (2002) Flow of activation from V1 to frontal cortex in humans: a framework for defining "early" visual processing. Exp Brain Res 142:39–150

Foxe JJ, Simpson GV (2005) Biasing the brain's attentional set. II. Effects of selective intersensory attentional deployments on subsequent sensory processing. Exp Brain Res 166:393–401

Foxe JJ, Simpson GV, Ahlfors SP (1998) Parieto–occipital 10 Hz activity reflects anticipatory state of visual attention mechanisms. NeuroReport 9:3929–3933

Foxe JJ, Doniger GM, Javitt DC (2001) Visual processing deficits in schizophrenia: impaired P1 generation revealed by high-density electrical mapping. NeuroReport 12(17):3815–3820

Foxe JJ, McCourt ME, Javitt DC (2003) Right hemisphere control of visuo-spatial attention: 'Line-bisection' judgments evaluated with high-density electrical mapping and source-analysis. NeuroImage 19:710–726

Foxe JJ, Murray MM, Javitt DC (2005a) Filling-in in schizophrenia: a high-density electrical mapping and source-analysis investigation of illusory contour processing. Cereb Cortex 15:1914–1927

Foxe JJ, Simpson GV, Ahlfors SP, Saron CD (2005b) Biasing the brain's attentional set. I. Cue driven deployments of intersensory selective attention. Exp Brain Res 166:370–392

Gitelman DR, Nobre AC, Parrish TB, LaBar KS, Kim YH, Meyer JR, Mesulam M (1999) A large-scale distributed network for covert spatial attention: further anatomical delineation based on stringent behavioural and cognitive controls. Brain 122(Pt 6):1093–1106

Givre SJ, Schroeder CE, Arezzo JC (1994) Contribution of extrastriate area V4 to the surface-recorded flash VEP in the awake macaque. Vision Res 34(4):415–428

Givre SJ, Arezzo JC, Schroeder CE (1995) Effects of wavelength on the timing and laminar distribution of illuminance-evoked activity in macaque V1. Vis Neurosci 12(2):229–239

Gomez-Gonzalez CM, Clark VP, Fan S, Luck SJ, Hillyard SA (1994) Sources of attention-sensitive visual event-related potentials. Brain Topogr 7:41–51

Guthrie D, Buchwald JS (1991) Significance testing of difference potentials. Psychophysiology 28(2):240–244

Hall SD, Holliday IE, Hillebrand A, Furlong PL, Singh KD, Barnes GR (2005) Distinct contrast response functions in striate and extra-striate regions of visual cortex revealed with magnetoencephalography (MEG). Clin Neurophysiol 116:1716–1722

Heilman KM, Van Den Abell T (1980) Right hemisphere dominance for attention: the mechanism underlying hemispheric asymmetries of inattention (neglect). Neurology 30:327–330

Hillyard SA, Anllo-Vento L (1998) Event-related brain potentials in the study of visual selective attention. Proc Natl Acad Sci 95: 781–787

Hillyard SA, Vogel EK, Luck SJ (1998) Sensory gain control (amplification) as a mechanism of selective attention: electrophysiological and neuroimaging evidence. Philos Trans R Soc Lond B Biol Sci 353:1257–1270

Hubel DH, Livingstone MS (1990) Color and contrast sensitivity in the lateral geniculate body and primary visual cortex of the macaque monkey. J Neurosci 10(7):2223–2237

Ikeda H, Nishijo H, Miyamoto K, Tamura R, Endo S, Ono T (1998) Generators of visual evoked potentials investigated by dipole tracing in the human occipital cortex. Neuroscience 84:723–739

Jeffreys DA, Axford JG (1972) Source locations of pattern-specific components of human visual evoked potentials. I. Component of striate cortical origin. Exp Brain Res 16:1–21

Kaiser PK (1979) Spectral sensitivity function measured by a rapid scan flicker photometric procedure. Invest Ophthalmol Vis Sci 18:1264–1272

Kaplan E (1991) The receptive field structure of retinal ganglion cells in cat and monkey. In: Cronly-Dillon J (ed) Vision and visual dysfunction, vol 4, AG Leventhal: the neural basis of visual function. CRC Press, Boca Raton, Florida, pp 10–40

Kaplan E, Shapley RM (1986) The primate retina contains two types of ganglion cells, with high and low contrast sensitivity. Proc Natl Acad Sci USA 83(8):2755–2757

Kelly SP, Gomez-Ramirez M, Foxe JJ (in press) Spatial attention modulates initial afferent activity in human primary visual cortex. Cerebral Cortex Advance Access published on March 4, 2008. doi:10.1093/cercor/bhn022

Kubová Z, Kuba M, Spekreijse H, Blakemore C (1995) Contrast dependence of motion-onset and pattern-reversal evoked potentials. Vision Res 35:197–205

Lachter J, Forster KI, Ruthruff E (2004) Forty-five years after Broadbent (1958): still no identification without attention. Psychol Rev 111(4):880–913

Lalor EC, Foxe JJ (in press) Biasing responsivity of the magnocellular and parvocellular visual pathways using the Visual Evoked Spread Spectrum Analysis technique (VESPA). Vision Res

Lalor EC, Pearlmutter BA, Reilly RB, McDarby G, Foxe JJ (2006) The VESPA: a method for the rapid estimation of a visual evoked potential. Neuroimage 32:1549–1561

Lalor EC, Kelly SP, Pearlmutter B, Reilly RB, Foxe JJ (2007) Isolating endogenous visuo-spatial attentional effects using the novel Visual Evoked Spread Spectrum Analysis (VESPA) technique. Eur J NeuroSci 26:3536–3542

Lalor EC, Yeap S, Reilly RB, Pearlmutter BA, Foxe JJ (2008) Dissecting the cellular contributions to early visual sensory processing deficits in schizophrenia using the VESPA evoked response. Schizophr Res 98:256–264

Livingstone M, Hubel D (1988) Segregation of form, color, movement, and depth: anatomy, physiology, and perception. Science 240(4853):740–749

Livingstone MS, Rosen GD, Drislane FW, Galaburda AM (1991) Physiological and anatomical evidence for a magnocellular defect in developmental dyslexia. Proc Natl Acad Sci 88(18): 7943–7947

Mangun GR, Hinrichs H, Scholz M, Mueller-Gaertner HW, Herzog H, Krause BJ, Tellman L, Kemna L, Heinze HJ (2001) Integrating electrophysiology and neuroimaging of spatial selective attention to simple isolated visual stimuli. Vision Res 41(10–11):1423–1435

Martinez A, Anllo-Vento L, Sereno MI, Frank LR, Buxton RB, Dubowitz DJ, Wong EC, Hinrichs H, Heinze HJ, Hillyard SA (1999) Involvement of striate and extrastriate visual cortical areas in spatial attention. Nat Neurosci 2:364–369

Martinez A, DiRusso F, Anllo-Vento L, Sereno MI, Buxton RB, Hillyard SA (2001) Putting spatial attention on the map: timing and localization of stimulus selection processes in striate and extrastriate visual areas. Vision Res 41(10–11):1437–1457

Maunsell JHR, Ghose GM, Assad JA, McAdams CJ, Boudreau CE, Noerager BD (1999) Visual response latencies of magnocellular and parvocellular LGN neurons in macaque monkeys. Vis Neurosci 16:1–14

McCourt ME, Foxe JJ (2004) Brightening prospects for "early" cortical coding of perceived luminance. NeuroReport 15:49–56

Merigan WH (1989) Chromatic and achromatic vision of macaques: role of the P pathway. J Neurosci 9(3):776–783

Merigan WH, Maunsell JR (1993) How parallel are the primate visual pathways? Annual Rev Neurosci 16:369–402

Molholm S, Ritter W, Murray MM, Javitt DC, Schroeder CE, Foxe JJ (2002) Multisensory auditory-visual interactions during early sensory processing in humans: a high-density electrical mapping study. Cogn Brain Res 14:121–134

Noesselt T, Hillyard SA, Woldorff MG, Schoenfeld A, Hagner T, Jancke L, Tempelmann C, Hinrichs H, Heinze HJ (2002) Delayed striate cortical activation during spatial attention. Neuron 35(3):575–587

Oldfield RC (1971) The assessment and analysis of handedness: the Edinburgh inventory. Neuropsychologia 9:97–113

Perrin F, Pernier J, Bertrand O, Giard MH, Echallier JF (1987) Mapping of scalp potentials by surface spline interpolation. Electroencephalogr Clin Neurophysiol 66(1):75–81

Schechter I, Butler PD, Zemon VM, Revheim N, Saperstein AM, Jalbrzikowski M, Pasternak R, Silipo G, Javitt DC (2005) Impairments in generation of early-stage transient visual evoked potentials to magno- and parvocellular-selective stimuli in schizophrenia. Clin Neurophysiol 116(9):2204–2215

Schroeder CE, Tenke CE, Arezzo JC, Vaughan HG Jr (1989) Timing and distribution of flash-evoked activity in the lateral geniculate nucleus of the alert monkey. Brain Res 477(1–2):183–195

Schroeder CE, Tenke CE, Givre SJ, Arezzo JC, Vaughan HG Jr (1991) Striate cortical contribution to the surface-recorded pattern-reversal VEP in the alert monkey. Vision Res 31(7–8): 1143–1157

Schroeder CE, Javitt DC, Steinschneider M, Mehta AD, Givre SJ, Vaughan HG Jr, Arezzo JC (1997) N-methyl-D-aspartate enhancement of phasic responses in primate neocortex. Exp Brain Res 114(2):271–278

Schroeder CE, Mehta AD, Givre SJ (1998) A spatiotemporal profile of visual system activation revealed by current source density analysis in the awake macaque. Cereb Cortex 8:575–592

Schroeder CE, Mehta AD, Foxe JJ (2001) Determinants and mechanisms of attentional modulation of neural processing. Front Biosci 6:D672–D684

Schwartz BD, Tomlin HR, Evans WJ, Ross KV (2001) Neurophysiologic mechanisms of attention: a selective review of early information processing in schizophrenics. Front Biosci 6:D120–D134

Shapley R, Kaplan E, Soodak R (1981) Spatial summation and contrast sensitivity of X and Y cells in the lateral geniculate nucleus of the macaque. Nature 292(5823):543–545

Simpson GV, Pfleiger ME, Foxe JJ, Ahlfors SP, Vaughan HG Jr, Hrabe J, Ilmoniemi RJ, Lantos G (1995a) Dynamic neuroimaging of brain function. J Clin Neurophysiol 12(5):1–18

Simpson GV, Foxe JJ, Vaughan HG Jr, Mehta AD, Schroeder CE (1995b) Integration of electrophysiological source analyses, MRI and animal models in the study of visual processing and attention. Electroencephalogr Clin Neurophysiol Suppl 44:76–92

Tenke CE, Schroeder CE, Arezzo JC, Vaughan HG Jr (1993) Interpretation of high-resolution current source density profiles: a simulation of sublaminar contributions to the visual evoked potential. Exp Brain Res 94(2):183–192

Tootell RB, Switkes E, Silverman MS, Hamilton SL (1988a) Functional anatomy of macaque striate cortex. II. Retinotopic organization. J Neurosci 8:1531–1568

Tootell RB, Hamilton SL, Switkes E (1988b) Functional anatomy of macaque striate cortex. IV. Contrast and magno-parvo streams. J Neurosci 8(5):1594–609

Tootell RB, Reppas JB, Kwong KK, Malach R, Born RT, Brady TJ, Rosen BR, Belliveau JW (1995) Functional analysis of human MT and related visual cortical areas using magnetic resonance imaging. J Neurosci 15(4):3215–3230

Tootell RB, Hadjikhani NK, Vanduffel W, Liu AK, Mendola JD, Sereno MI, Dale AM (1998) Functional analysis of primary visual cortex (V1) in humans. Proc Natl Acad Sci USA 95(3): 811–817

Ungerleider LG, Mishkin M (1982) Two cortical visual systems. In: Ingle DJ, Goodale MA, Mansfield RJW (eds) Analysis of visual behavior. MIT Press, Cambridge, MA, pp 549–585

Vallar G, Perani D (1986) The anatomy of unilateral neglect after right-hemisphere stroke lesions: a clinical/CT-scan correlation study in man. Neuropsychologia 24:609–622

Vallar G, Perani D (1987) The anatomy of spatial neglect in humans. In Jennerod (ed) Neurophysiological and neuropsychological aspects of spatial neglect. North Holland, Amsterdam, pp 235–258

Van Essen DC, Maunsell JHR (1983) Hierarchical organization and functional streams in the visual cortex. Trends Neurosci 6:370–375

Yeap S, Kelly SP, Sehatpour P, Magno E, Javitt DC, Garavan H, Thakore JH, Foxe JJ (2006) Early visual sensory deficits as endophenotypes for Schizophrenia: high-density electrical mapping in clinically unaffected first-degree relatives. Arch Gen Psychiatry 63:1180–1188